BeBeC-2018-S05

IMPROVING SOURCE LOCALISATION WITH SODIX FOR A SPARSE MICROPHONE ARRAY

Sebastian Oertwig[1], Stefan Funke[2] and Henri Siller[1]
[1]German Aerospace Center (DLR), Institute of Propulsion Technology, Engine Acoustics Department
Müller-Breslau-Str. 8, 10623 Berlin, Germany
[2]Rolls-Royce Deutschland Ltd. & Co KG
Eschenweg 11, OT Dahlewitz, 15827 Blankenfelde-Mahlow, Germany

Abstract

SODIX is an acoustic source localisation method that is able to resolve the directivity of the sound sources. In this paper, SODIX is applied to array measurements with a full-scale turbofan engine. Two different microphone arrays were used: 1) a linear array near the engine that was relatively densely populated with a total number of 248 microphones, and 2) a sparse microphone array in the far-field with only 31 microphones covering an angular range from 10° to 160°. The source localisation results obtained from the analysis of both arrays are compared and it will be shown, that also the sparse array yields very good results. One free parameter in the SODIX algorithm is a penalty function that sets a constraint on the directivities of the sources, i.e. the amplitude changes from a single source to different microphones. The influence of this penalty function on the quality of the results is investigated on the basis of the experimental data and synthetic data generated from a relatively simple engine noise model. A practical improvement for the setup of the sparse far-field microphone array is proposed for future measurements.

1 INTRODUCTION

The sound field emitted by turbofan engines and their components is highly directional. Conventional source localisation methods such as *beamforming* can only provide limited results because they rely on the assumption of monopole sources with uniform directivity. A method that is capable of determining the directivities of the sound sources is the *SOurce DIrectivity modelling in the cross-spectral matriX (SODIX)*. This method fits a model of the cross-spectral matrix to measured data from a microphone array by assuming incoherent point sources with individual directivity towards each microphone.

SODIX was compared to various advanced deconvolution methods for an experimental setup with uniform monopole sources [5]. The method showed a similar resolution and dynamic range despite the much higher number of unknowns to be determined. The great advantage of SODIX is the capability of determining the directivities of sound sources which is important for highly directional sound sources, as e.g. turbofan engines.

The localisation method SODIX was developed at DLR for the analysis of the highly directional sound fields in static aero-engine noise tests [5, 7, 10]. A common setup for these free-field engine tests consists of a large microphone array in parallel with the engine axis. DLR uses a linear array that is densely populated with up to 248 microphones [4]. The source localisation with such a microphone array is able to resolve the individual far-field characteristics of the main source regions intake, nozzle, and jet [4].

During static engine noise tests, microphones are usually installed in a circular arrangement in the far-field for the purpose of noise certification according to SAE ARP1846A [1]. Compared to the large, linear microphone array, this array is sparsely populated with approximately 30 microphones. The application of SODIX to the data of the sparse far-field array promises substantial benefits in terms of both, reduced computational time and complexity of the setup. In this case, a reduction of the computation time by a factor of 20 can be achieved due to the lower microphone count at the cost of a lower spatial resolution. Most of all, the localisation with the far-field array is a new practical application since the data is available for each certified turbofan engine. Nevertheless, the feasibility of the source localisation with SODIX for a sparse microphone array has not been studied yet.

SODIX uses a penalty function that sets a constraint on the amplitude changes from a single source to different microphones. The penalty function can help to improve the localisation results for ill-posed problems, as they can occur for sparse microphone arrays. Although there is some empirical experience on the weighting of the penalty function for the dense microphone array at static engine tests, the impact on source localisation with SODIX is not well understood. Therefore, the focus of this paper is on the source localisation with a sparse microphone array at static engine tests and the influence of applying a penalty function within the localisation algorithm. First, the localisation method SODIX is applied to data from the sparse microphone array. In this case, parameters of the penalty function are used that were empirically scaled from the application to a dense array such that similar effects on the source localisation are achieved. The results are compared to the localisation with a dense array in the near-field. Additionally, a variation of the parameters of the penalty function is examined for the sparse microphone array. Furthermore, this paper presents a parametric study of the penalty function for synthesised sound sources. The study is carried out on a simple engine noise model that models the directional source amplitudes of a jet engine perceived by the sparse far-field array. The success of the source localisation with varying parameters of the penalty function will be evaluated by the far-field characteristics of the sound sources calculated with SODIX.

2 METHODOLOGY

2.1 Source localisation method SODIX

SODIX is a source localisation method that is capable of determining the directivities of sound sources. The method was developed by Funke and Michel [4, 5, 7, 10] as an extension of the

Spectral Estimation Method (SEM) by Blacodon and Élias [2, 3]. The localisation strategy is based on the modelling of the measured cross-spectral matrix C_{mn} from microphone signals. The model of the cross-spectral matrix consists of incoherent point sources D_{jm} with individual source amplitudes from all sources $j = 1 \ldots J$ towards all microphones $m = 1 \ldots M$ of the array:

$$C_{mn}^{\mathrm{mod}} = \sum_{j=1}^{J} g_{jm} D_{jm} D_{jn} g_{jn}^{*} \, . \tag{1}$$

In this model, g_{jm} represents the steering vector for the source j to the microphone m. Although the steering vectors can be chosen freely within SODIX, in this paper the convenient assumption of free-field propagation is used:

$$g_{jm} = \frac{1}{r_{jm}} e^{ikr_{jm}} \, , \tag{2}$$

where r_{jm} is the distance from source j to the microphone m, and k is the wave number. The directional amplitudes of the sources D_{jm} are calculated by a least-squares fit between the measured and the modelled cross-spectral matrix:

$$F(D) = \sum_{m,n=1}^{M} \left| C_{mn} - C_{mn}^{\mathrm{mod}} \right|^2 \, . \tag{3}$$

With Eq. (1), this formulation leads to an optimisation problem for the source amplitudes D_{jm}. The cost function F between measured and modelled cross-spectral matrix is minimised by a conjugate gradient method. A constraint on the minimisation consists in positive source amplitudes $D_{jm} \geq 0$ which can be fulfilled by substituting $D_{jm} = d_{jm}^2$ in the modelling of the cross-spectral matrix [7]. It can be shown that the solution for the new cost function $F(d)$ is equal to the solution with the original statement for D_{jm} if the initial guess is rather smooth. In general, a constant source distribution based on the measured sound pressure level of each microphone $d_{jm^*} = \text{const.}$ with $m^* = 1 \ldots M$ is used as start solution for the optimisation.

2.2 Applying a penalty function in SODIX

The parametric optimisation leads to source directivities that are $D \in \mathbb{R}_{+}^{J \times M}$ where J is the source number and M is the microphone count. The dimension of the measured cross-spectral matrix is $C_{mn} \in \mathbb{C}^{(M^2+M)/2}$ (only independent values). For large source grids or sparse microphone arrays, the minimisation of the cost function as stated in Eq. (3) might be ill-posed. Therefore, a penalty function is introduced to the cost function that allows to solve the minimisation problem for applications with more unknown directivities D_{jm} than independent entries in the measured cross-spectral matrix C_{mn}:

$$F(D) = \sum_{m,n=1}^{M} \left| C_{mn} - C_{mn}^{\mathrm{mod}} \right|^2 + \sigma_{\mathrm{d}} G_{\mathrm{d}} \, , \tag{4}$$

with the penalty function G_d and the penalty coefficient σ_d. The main idea of the penalty function within the localisation method SODIX relies on the local smoothness of the source directivities. It is assumed that the directivities for each source are rather smooth in a local domain leading to the following scheme for the penalty function:

$$G_\mathrm{d}(D) = \sum_{j=1}^{J} \sum_{m=1}^{M} \sum_{l=1}^{L(m)} \alpha_l \left(D_{jm} - D_{j,\Lambda(l)} \right)^2 . \tag{5}$$

In this strategy, the source directivity D_{jm} for a particular source j in direction to a microphone m is determined by including the directivities of the same source j within a certain domain. L stands for the number of nearby microphones that are taken into account in the penalty function. The coefficient α_l represents a linear weighting of the considered directivities within the domain with the corresponding distances r:

$$\alpha_l = 1 - \frac{r(l)}{r_m} . \tag{6}$$

As a generalised approach, a spherical domain is used to determine neighboured microphones. This approach enables the universal usage of the scheme for complex microphone arrangements and source grids. In practice, the number of microphones that is considered for the penalty function is set by the parameter *angular aperture* G_ϕ in degree, see also [4]. For large values of this parameter, SODIX considers a larger domain for neighboured microphones in the penalty function.

Figure 1 compares the source localisation with SODIX with and without the penalty function applied for a generic study.

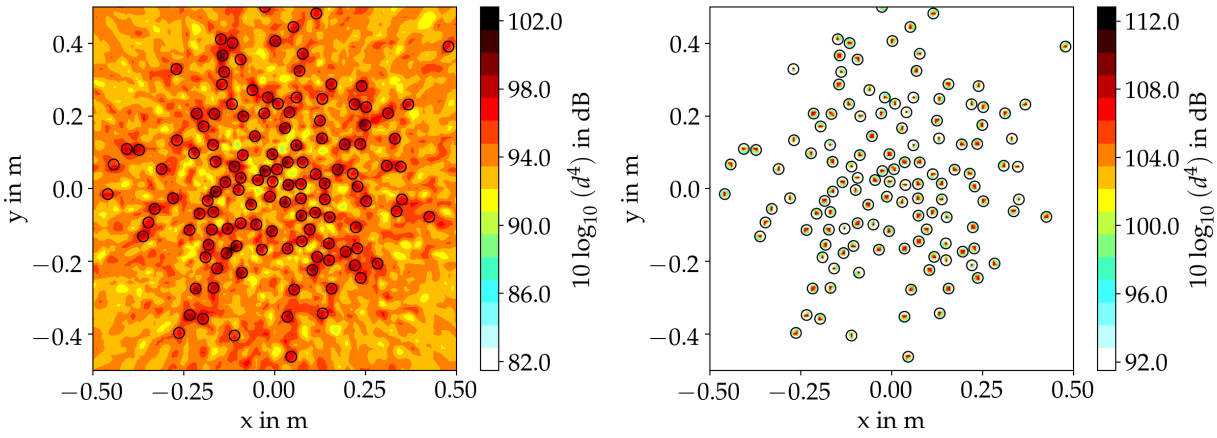

(a) w/o penalty function applied

(b) w penalty function applied

Figure 1: Simulation of 128 monopole sources perceived by a spiral array with 64 microphones. The maps show the source amplitudes determined with SODIX without (left) and with (right) penalty function applied. Both source maps show a dynamic range of 20 dB. The peak level increases by 10 dB when the penalty function is applied, but the overall power resumes preserved. Black circles indicate the simulated source positions.

The sound field is synthesised with 128 equally strong monopoles with a spatial Gaussian distribution. The simulation frequency is 10880 Hz and the sources are separated by at least one wavelength. The radius of the black circles in Fig. 1 that indicate the source positions is 0.5 of the wavelength. The signals are simulated for a spiral array with only 64 microphones, see [9], at a distance of one metre to the source plane. SODIX uses a rectangular grid that consists of 10404 points with an equidistant spacing of 0.32 of the wavelength. In this case, the number of unknown directional source amplitudes of 665856 is much higher than the number of independent values in the cross-spectral matrix of 2080. Hence, this problem is ill-posed and the localisation without the penalty function applied results in a source map with rather low dynamic range. The source positions are not accurately detected. Applying the penalty function increases the dynamic range of the solution derived by SODIX. All synthesised point sources can be separated well. This simulation gives a first indication that the source localisation method SODIX is able to work with sparse microphone arrays for an academic example. The influence of the penalty function on a real application will be investigated in this paper.

As a summary, the localisation method SODIX can be influenced by a penalty function and its two parameters, the penalty coefficient σ_d that is used to weight the penalty function against the raw source localisation and the angular aperture G_ϕ that controls the number of nearby microphones that are taken into account in the penalty function.

2.3 SODIX source map and far-field extrapolation

The SODIX results for one-dimensional source grids as used in this paper will be presented in source maps, as shown in Fig. 2.

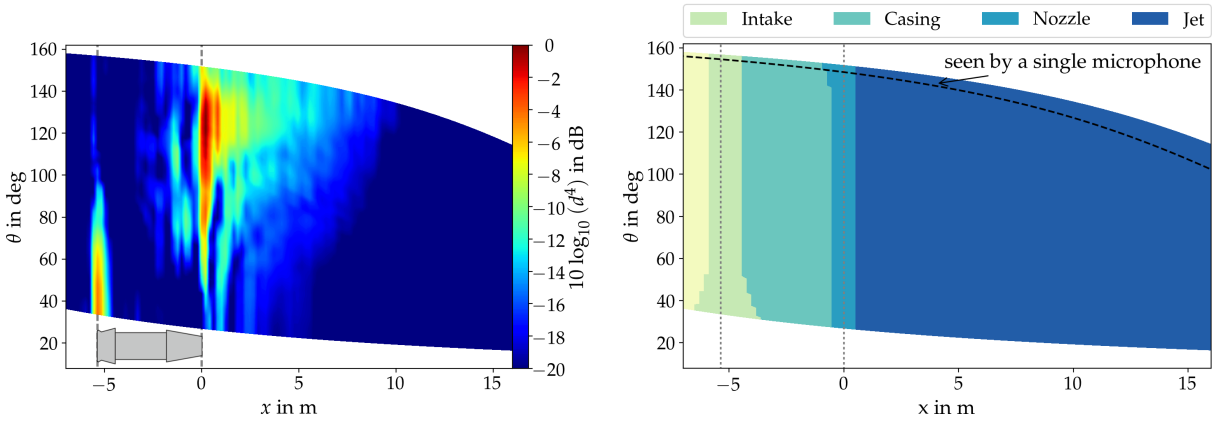

(a) SODIX source map derived from a dense array

(b) Areas for source breakdown

Figure 2: Source localisation with SODIX with a dense microphone array for a turbofan engine and source breakdown areas intake, casing, nozzle, and jet for far-field extrapolation for the 400 Hz one-third octave band. The directivity of each source position is shown on the vertical axis. The dashed grey lines represent the axial positions of engine intake and nozzle. The black curve represents the source directivities seen by a single microphone.

These maps show the source strengths for an emission angle on the vertical axis and the source position (of the engine axis) given on the horizontal axis. The individual directivities of a single sound source can be read vertically, see e.g. the grey dashed lines for intake and nozzle position. In this context, the emission angle is defined by the line from a source to a microphone and the engine axis. Flight coordinates are used so that an emission angle of 0° points in flight direction, whereas 180° is in jet direction. In this meaning, the emission angle is a local property of each source and varies with the source position for a particular microphone, see the dashed black line in Fig. 2.

The source distribution calculated with SODIX can be extrapolated to the far-field in order to compare the sound emission with reference microphones in the far-field and evaluate the contribution of the single source regions to overall far-field levels. In general, free-field steering vectors as in Eq. (2) are used to perform the extrapolation for the individual source amplitudes. The source areas intake, casing, nozzle, and jet are obtained by a geometric source breakdown, as shown in Fig. 2. The source areas corresponding to the intake and the nozzle broaden for small and large emission angles respectively to account for parallax effects due to the one-dimensional source grid [4], whereas the physical radiation areas are distributed off-axis. To compare the extrapolated SODIX results with far-field measurements, a global polar angle is defined with the centre point on the engine nozzle.

3 APPLICATION TO MEASURED ENGINE DATA

3.1 Experimental setup at static free-field aero-engine noise tests

Figure 3 shows two different microphone setups that were used during static free-field tests with a long cowl turbofan engine at the Rolls-Royce test facility in Mississippi (USA) in 2011 [6].

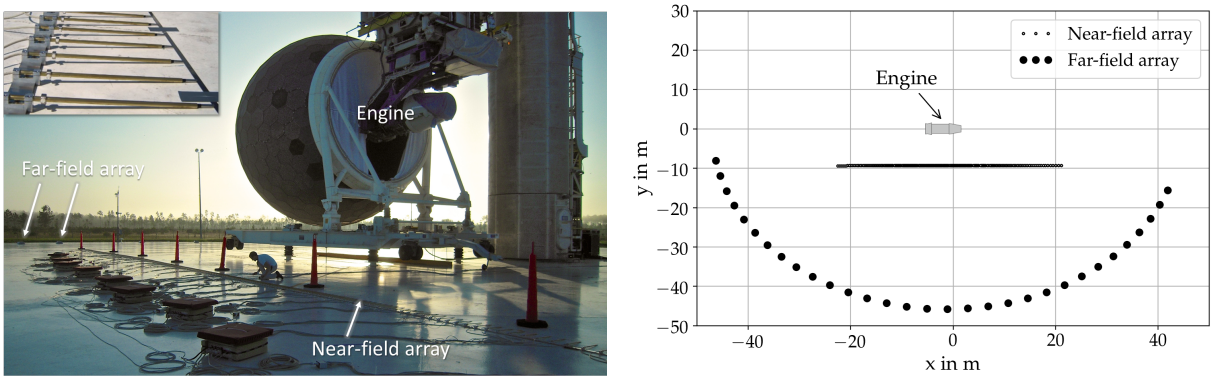

(a) Measurement setup at static engine tests [4]

(b) Microphone positions for both setups

Figure 3: Measurement setup with microphone arrays at a static free-field engine test stand. The dense near-field array consists of 248 microphones arranged in a line parallel to the engine axis with a polar resolution of 0.6°. The sparse circular array in the far-field consists of 31 microphones with a polar resolution of 5°.

The dense array near the engine consists of 248 microphones that are arranged in a line in parallel with the engine axis. The lateral distance of the microphone array to the engine axis

is approximately 10 m. The engine was mounted with the engine centreline 6.4 m above the ground plane. The large microphone array in the geometric near-field provides a constant polar resolution of 0.6°.

In comparison, the sparse microphone array consists of only 31 microphones that are located in the far-field of the engine. The microphones are arranged in a circle with a constant polar resolution of 5° from 10° to 160° at a distance of 150 ft (45.72 m) to the engine centre. Such a far-field microphone setup is normally used for certification purposes of aircraft engines [1].

3.2 Source localisation at static engine tests

Figure 4 compares the source localisation with SODIX for the dense array on the left-hand side and for the sparse far-field array on the right-hand side in the one-third octave bands 200 Hz, 400 Hz and 800 Hz respectively. As a first approach to show the general feasibility of the source localisation with the reduced array, the parameters of the penalty function from the dense array ($\sigma_\mathrm{d} = 1$, $G_\phi = 3°$) were empirically scaled for the application to the far-field array ($\sigma_\mathrm{d} = 0.01$, $G_\phi = 6°$) such that a similar effect on the results is achieved.

The source localisation for the intake and the nozzle area is in good agreement for both microphone arrays, see the grey dashed lines at intake and nozzle position. The far-field array even provides a wider angular range which leads e.g. in the intake area to a better detection of the maximum directivity at small emission angles. Nevertheless, the source map derived from the far-field array includes spurious sound sources in the downstream area from 400 Hz on. The sources downstream the nozzle position ($x > 0$ m) are moved to positions further downstream when localised with the sparse array. This phenomenon seems unreliable and might occur due to the spatial undersampling with the sparse far-field array. The microphone separation in this array is 4 m, whereas the wavelength in the 400 Hz one-third octave band is less than one metre.

A direct comparison of the localisation results from both microphone arrays can be achieved by the extrapolation of the individual sources to the far-field. Therefore, Fig. 5 depicts the far-field characteristics of the source regions intake, casing, nozzle, and jet that were derived by a geometric source breakdown, see Fig. 2, and extrapolation of the SODIX results shown in Fig. 4. The coloured lines show the sound pressure level for the corresponding source areas over the polar angle. The overall sound pressure level calculated with SODIX (black line) is compared to the measured data in the far-field (circles).

The source localisation with the dense microphone array in the near-field is capable of determining the directivities of the main source regions. As expected, the sound from the intake area radiates mainly upstream whereas nozzle and jet sources radiate downstream, e.g. for 800 Hz the maximum directivity for the jet is at polar angles of 125° and for the nozzle at 115°. The dynamic range of the source localisation with the dense array is approximately 20 dB, which is illustrated by the constant curve of the intake source at high emission angles. The overall sound pressure level derived by SODIX from the near-field array is in good agreement with the measured data in the far-field.

The far-field characteristics of the individual source regions for the sparse array are in good agreement with the results from the near-field array. The directivities of intake, nozzle, and jet can be reproduced with the sparse microphone array. The results prove the capability of the source localisation method SODIX to work with the data from the sparse far-field array despite the low number of microphones. Nevertheless, the usage of the far-field array leads to a source localisation with less dynamic range. This phenomenon can be seen e.g. for the

intake source at high polar angles in the rear arc. The dynamic range of more than 20 dB for the dense array decreases to 10 dB for the far-field array. Despite the spurious sound sources in the source maps, the impact of the sparse microphone array on the far-field directivity of nozzle and jet is rather low. The maximum levels for nozzle and jet differ 1-2 dB for both array configuration. The overall sound pressure levels derived by SODIX match even better with the measured far-field levels since the same signals from the far-field array were processed in this case. In general, the comparison of the overall sound pressure level with the measured data shows that the optimisation process in SODIX is energy conserving, see Eq. (3).

It is concluded that a source localisation with the sparse microphone array in the far-field is feasible although spurious sound sources downstream of the jet area might originate from the low spatial sampling of the sound field by the far-field array. If this phenomenon can be reduced or even eliminated by applying a penalty function with optimised parameters will be further discussed.

Figure 6 and Fig. 7 show the localisation results for the application of SODIX to the data of the far-field array for different parameter combinations of the penalty function. Figure 6 depicts the results for a variation of the parameter σ_d, whereas Fig. 7 presents those for a variation of the parameter G_ϕ. To allow a better comparison, also the raw source localisation without the penalty function applied is shown.

The spurious sound sources downstream the jet area occur for all parameter combinations examined. The variation of the penalty coefficient σ_d for the empirical value $G_\phi = 6^\circ$ has no impact on this phenomenon. The unreliable sources remain downstream the jet area whether the penalty function is applied. High values of the parameter σ_d smoothen the directivities in the far-field and the far-field characteristics become unreliable uniform. It is concluded that $\sigma_\mathrm{d} = 0.01$ is a good choice for the application of SODIX to the far-field data.

The same influence can be noticed for the parameter G_ϕ which controls the number of microphones that are taken into account in the penalty function. High values of this parameter cause similar effects as the penalty coefficient such that the far-field characteristics become unreliable uniform. Nevertheless, a reduction of the spurious sound sources in the jet area can be achieved with a slightly larger value $G_\phi = 10$ compared to the empirical value $G_\phi = 6$. It can be concluded that the parameter combination $\sigma_\mathrm{d} = 0.01$ and $G_\phi = 10$ appears to be a good, practical choice for the penalty function in SODIX for this specific application.

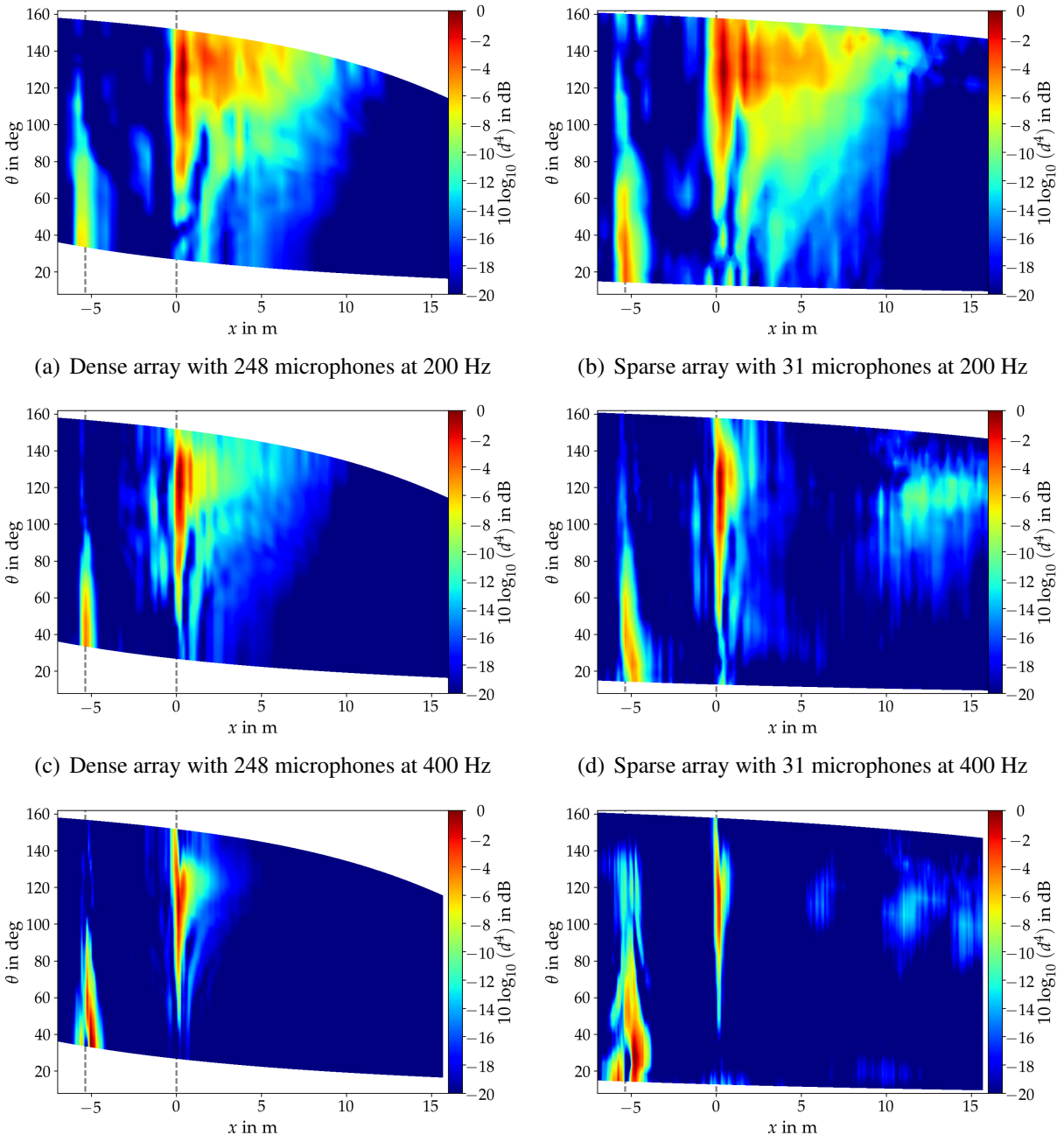

(a) Dense array with 248 microphones at 200 Hz

(b) Sparse array with 31 microphones at 200 Hz

(c) Dense array with 248 microphones at 400 Hz

(d) Sparse array with 31 microphones at 400 Hz

(e) Dense array with 248 microphones at 800 Hz

(f) Sparse array with 31 microphones at 800 Hz

Figure 4: Comparison of the source localisation with SODIX for a turbofan engine with a dense (left) and a sparse microphone array (right) for different one-third octave bands. The source position on the engine axis is given on the horizontal axis. The directivity of each source is shown on the vertical axis. The dashed lines represent the positions of the engine intake and nozzle. Empirical parameters of the penalty function were used.

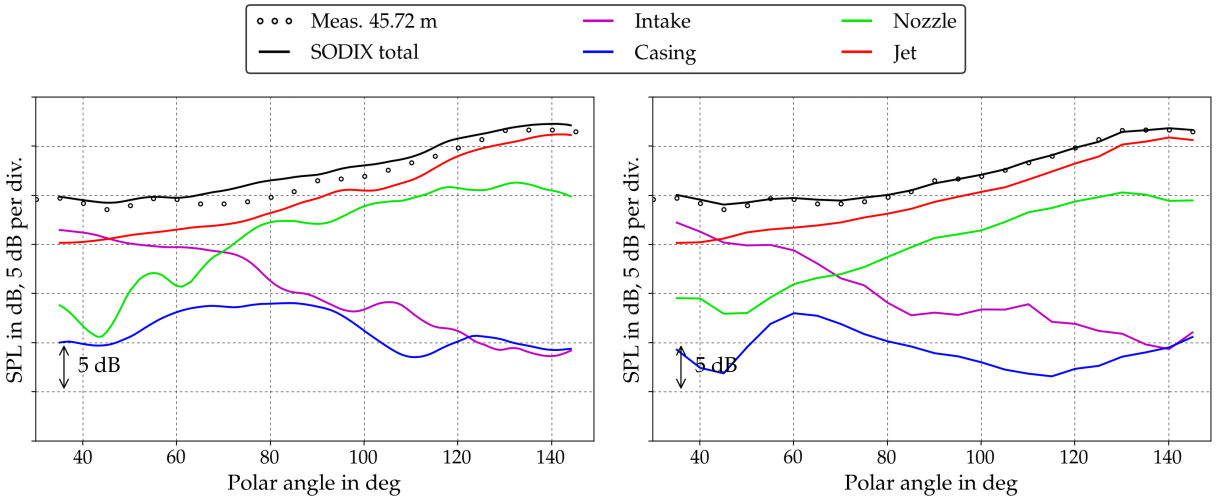

(a) Dense array with 248 microphones at 200 Hz

(b) Sparse array with 31 microphones at 200 Hz

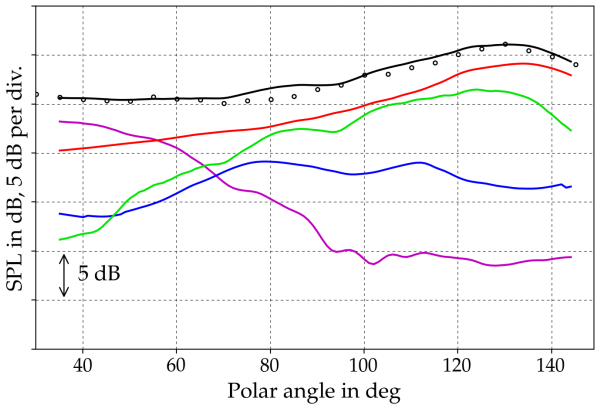

(c) Dense array with 248 microphones at 400 Hz

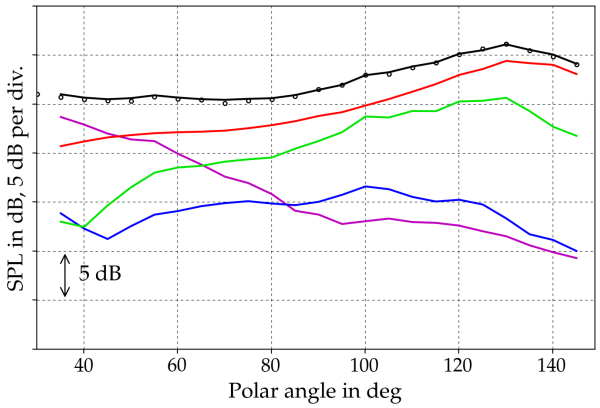

(d) Sparse array with 31 microphones at 400 Hz

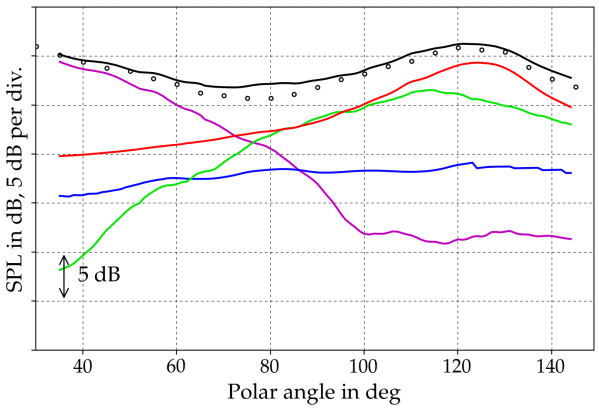

(e) Dense array with 248 microphones at 800 Hz

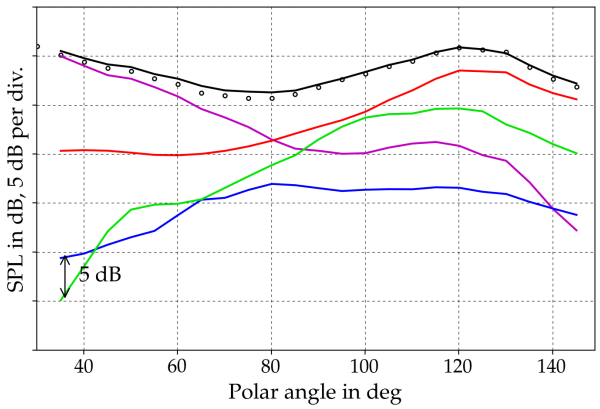

(f) Sparse array with 31 microphones at 800 Hz

Figure 5: Comparison of the far-field extrapolation of the source localisation with SODIX for a turbofan engine with a dense (left) and a sparse microphone array (right) for different one-third octave bands. Empirical parameters of the penalty function were used.

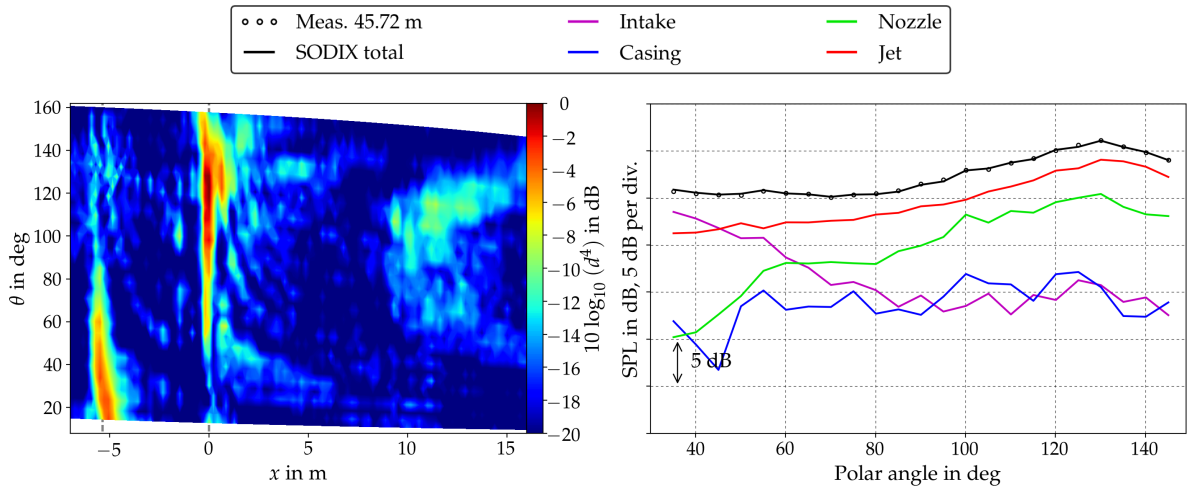

(a) w/o penalty function applied ($\sigma_\mathrm{d} = 0$, $G_\phi = 0°$)

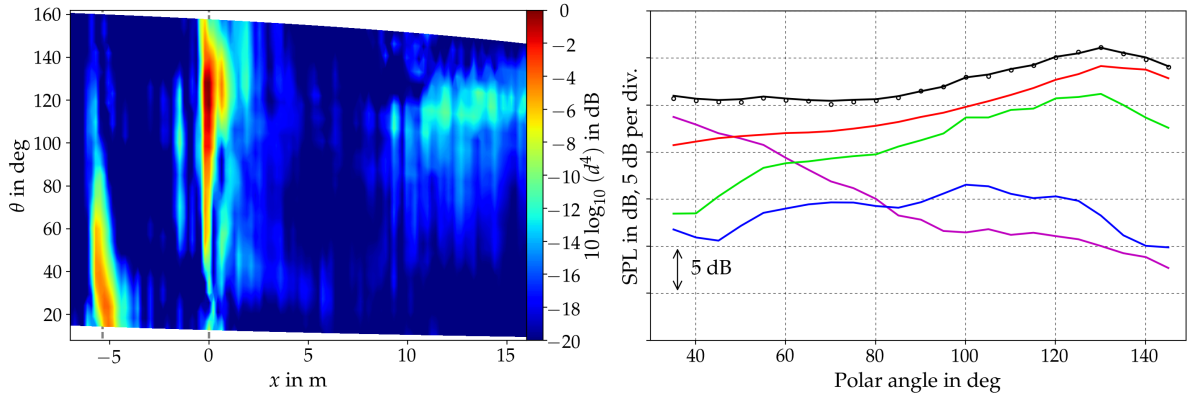

(b) w penalty function applied ($\sigma_\mathrm{d} = 0.01$, $G_\phi = 6°$)

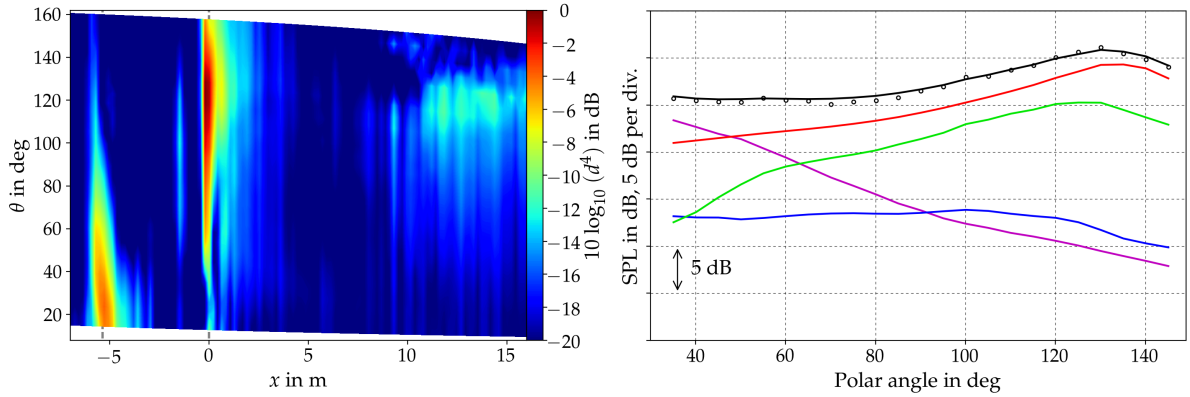

(c) w penalty function applied ($\sigma_\mathrm{d} = 0.10$, $G_\phi = 6°$)

Figure 6: Influence of the parameters of the penalty function on source localisation with SODIX and far-field extrapolation for a turbofan engine with a sparse microphone array in the 400 Hz one-third octave band - no penalty function applied (top) and different values of σ_d for constant G_ϕ.

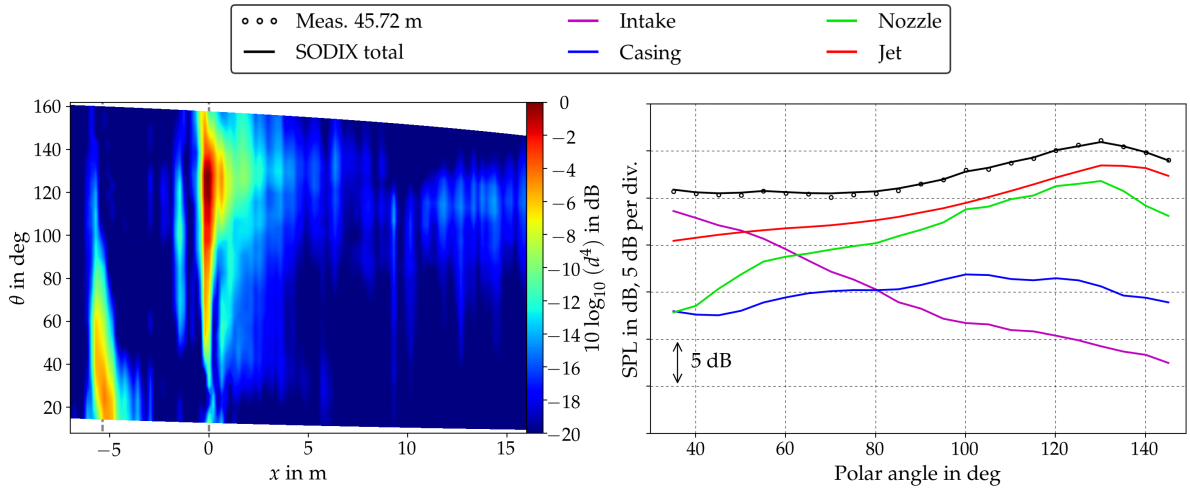

(a) w penalty function applied ($\sigma_\mathrm{d} = 0.01$, $G_\phi = 10°$)

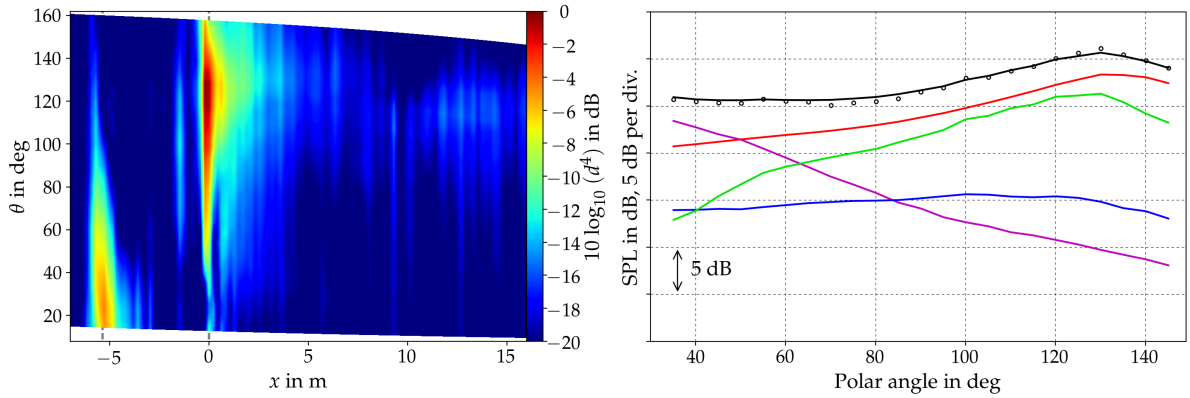

(b) w penalty function applied ($\sigma_\mathrm{d} = 0.01$, $G_\phi = 15°$)

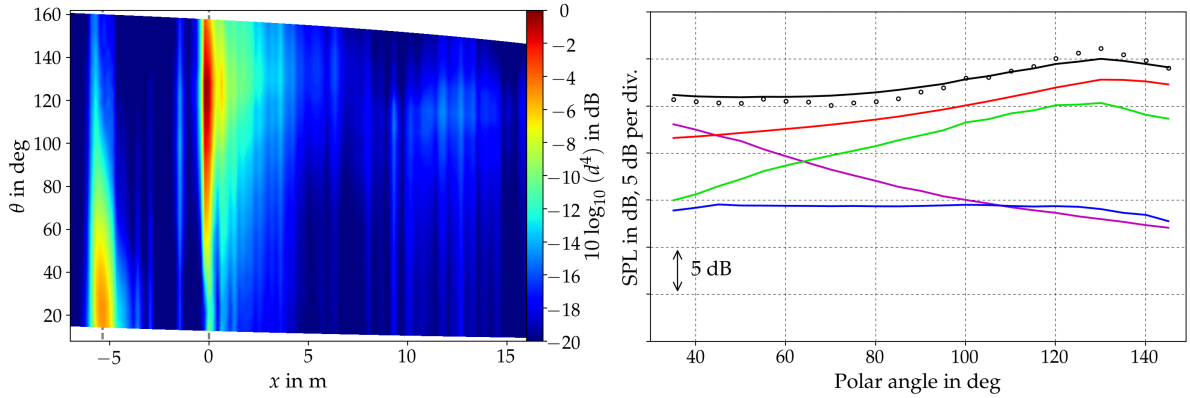

(c) w penalty function applied ($\sigma_\mathrm{d} = 0.01$, $G_\phi = 25°$)

Figure 7: Influence of the parameters of the penalty function on source localisation with SODIX and far-field extrapolation for a turbofan engine with a sparse microphone array in the 400 Hz one-third octave band - different values of G_ϕ for constant σ_d.

4 APPLICATION TO SIMULATED DATA

4.1 Sound field simulation with a simple engine noise model

Although the derived directivities of the main source regions can be compared to analytical models, the evaluation of the source localisation of real turbofan engines, specifically the source breakdown, is rather complex. Hence, a benchmark case is useful to investigate the localisation properties of SODIX, as e.g. the influence of the penalty function. A simple simulation with directional point sources is presented in this paper to account for the advantages of the localisation method SODIX. The test case models the cross-spectral matrix for the source areas intake, casing, nozzle, and jet based on the SODIX model, see Eq. (1). This test case is a very simplified model for the sound emission of a real turbofan engine and its only purpose is to demonstrate the capabilities of SODIX rather than to provide a model of the sound emission from aero-engines. Figure 8 depicts the source amplitudes and the corresponding directivities for the source regions intake, casing, nozzle, and jet.

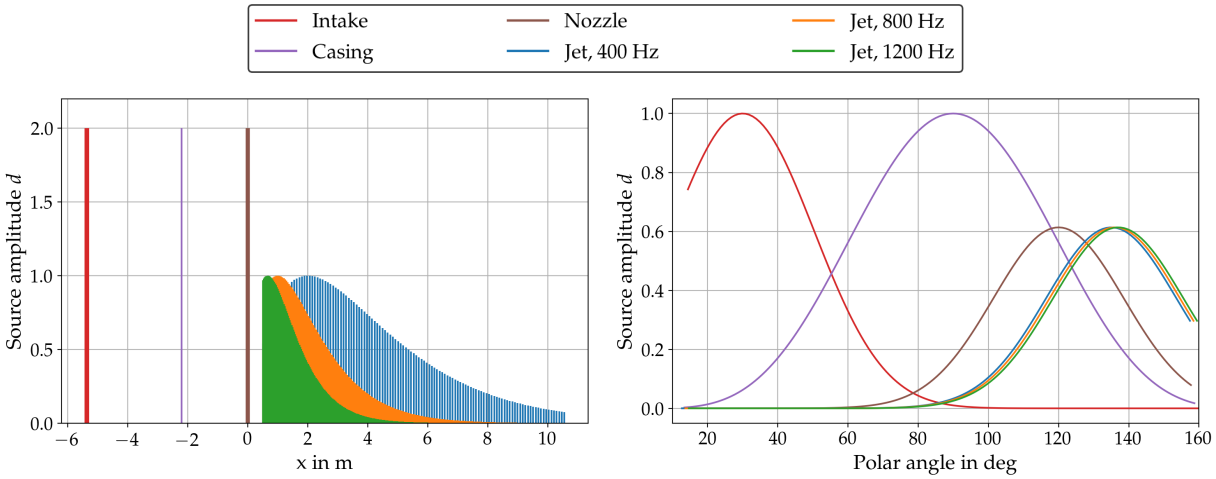

(a) Source amplitudes over source position

(b) Source directivities over polar angle

Figure 8: Source amplitudes and source directivities for a simple engine noise model based on point sources on the engine axis. The intake and the nozzle are modelled by three incoherent point sources that are separated by one twentieth of the wavelength. The jet noise is modelled by a line of point sources with frequency dependent position of the maximum amplitude.

The point sources are located on the engine axis where $x \approx -5.4$ m represents the position of the engine intake and $x = 0$ m is at the nozzle exit. The sound fields from the intake and the nozzle are each described by three individual point sources that are separated one twentieth of the wavelength respectively. The jet is modelled by an analytical source distribution on the engine axis with a frequency dependent source position of the maximum amplitude as described by Glegg [8]. Additionally, a single point source with rather small amplitude is simulated on the engine casing between intake and nozzle. The directivity of the intake sources is generated by a sinusoidal function with maximum intensity at polar angles of 30°. The directivity of the nozzle sources is given by a Gaussian distribution that radiates with maximum intensity at polar

angles of 120°. The jet directivity is assumed to be frequency independent with a maximum level at 135°. The additional source on the casing is simulated with a sinusoidal directivity with maximum level at polar angles of 90°. No further background noise is included in this study. Equation (7) shows the corresponding model of the cross-spectral matrix for the intake source:

$$C_{mn}^{\text{mod, Intake}} = \sum_{j=1}^{J} g_{jm} d_{jm}^2 d_{jn}^2 g_{jn}^* \quad \text{with} \quad d_{jm} = A \cos^4\left(\frac{\theta}{2} - \frac{30^\circ}{2}\right) . \tag{7}$$

4.2 Parametric study of the penalty function

A simple engine noise model is used to study the influence of the penalty function on the source localisation with SODIX. The calculations were performed varying both parameters, the angular aperture G_ϕ and the penalty coefficient σ_d. The localisation results derived by SODIX can be compared to the simulated data. To do this, the far-field characteristics of the individual source regions intake, casing, nozzle, and jet were integrated over all emission angles. The differences between the localisation results and the simulated data were normalised with the SODIX results without the penalty function applied. Figure 9 shows the results for the examined parameter field. The bottom row ($G_\phi = 0$) in Fig. 9 represents the localisation without the penalty function applied and equals 0 dB due to the normalisation. The best parameter combination found for each source area is marked by a pink square, respectively.

High values of the penalty coefficient σ_d lead to far-field characteristics that do not match the reference values of the simulation as the SODIX results without applying the penalty function. For the raw source localisation without the penalty function, the overall level is 3 dB lower for all source areas. For the source regions casing, nozzle, and jet, this effect takes over when the penalty coefficient reaches $\sigma_\mathrm{d} = 0.005$. The influence of the parameter G_ϕ is much weaker in the examined parameter field. Although the optimum parameter combination varies for each source region, a certain range of the parameters can be determined that provides the same improvement compared to the source localisation without the penalty function applied. Nevertheless, the improvement due to the penalty function varies for the different source areas, e.g. the intake far-field distribution can be improved by 3 dB with the penalty function whereas it has only a small effect on the far-field characteristics of the casing and the jet. Generally, it can be concluded from this study that the optimum parameter combination for the penalty function in SODIX depends mainly on the strength and directivity of the sources.

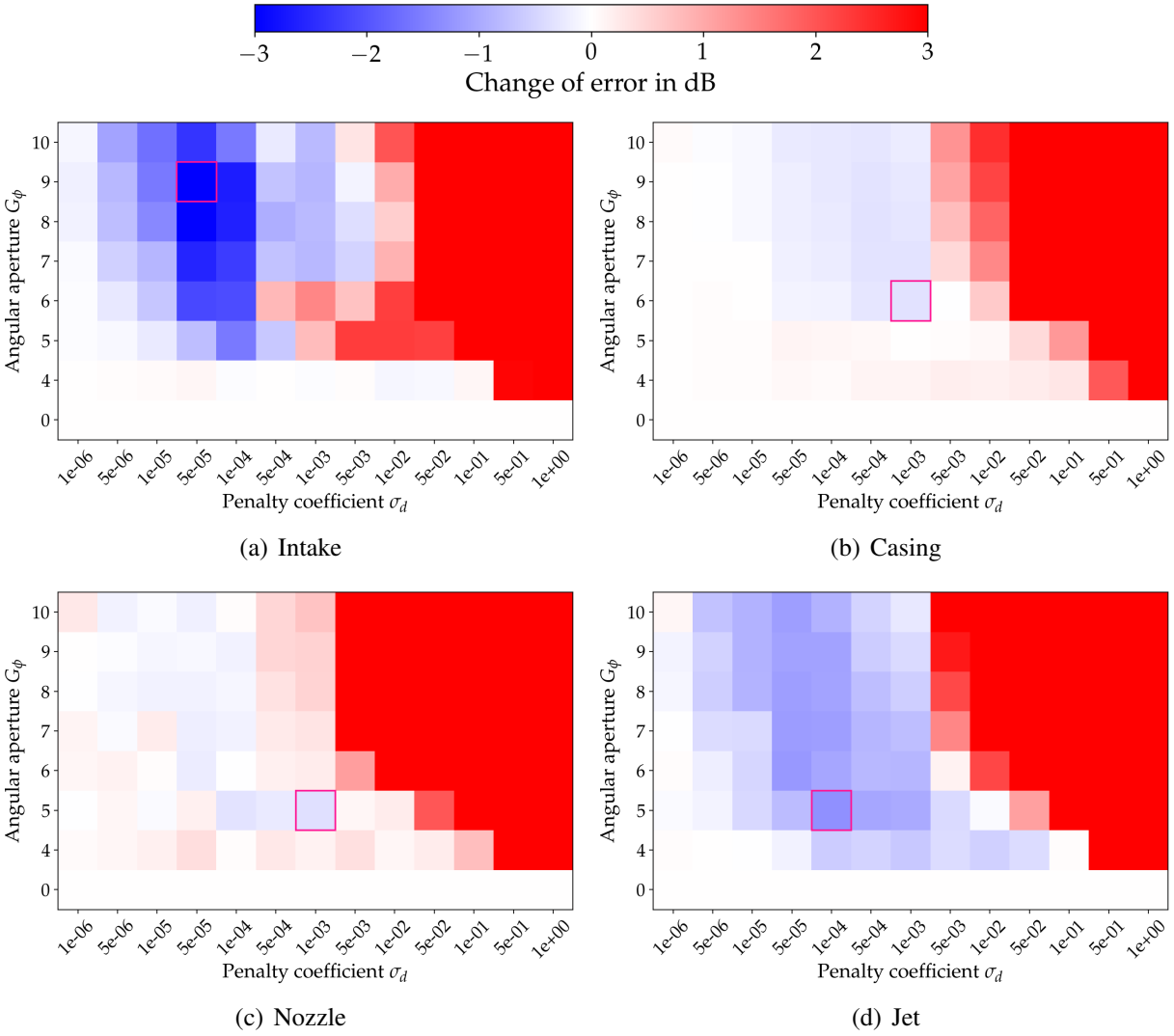

(a) Intake

(b) Casing

(c) Nozzle

(d) Jet

Figure 9: Parametric study of the penalty function in SODIX. The difference between simulation input and SODIX solution for the simulated data compared to localisation without the penalty function applied is shown. The best parameter combination found is marked by the pink square.

4.3 Improvement of the far-field array

The simulation data presented in section 4.1 will be used to investigate a possible extension of the sparse far-field array. As seen in section 3.2, the spatial undersampling by the far-field array leads to spurious sources in the rear arc. Therefore, an extension of the microphone array in the rear arc is proposed that is shown in Fig. 10.

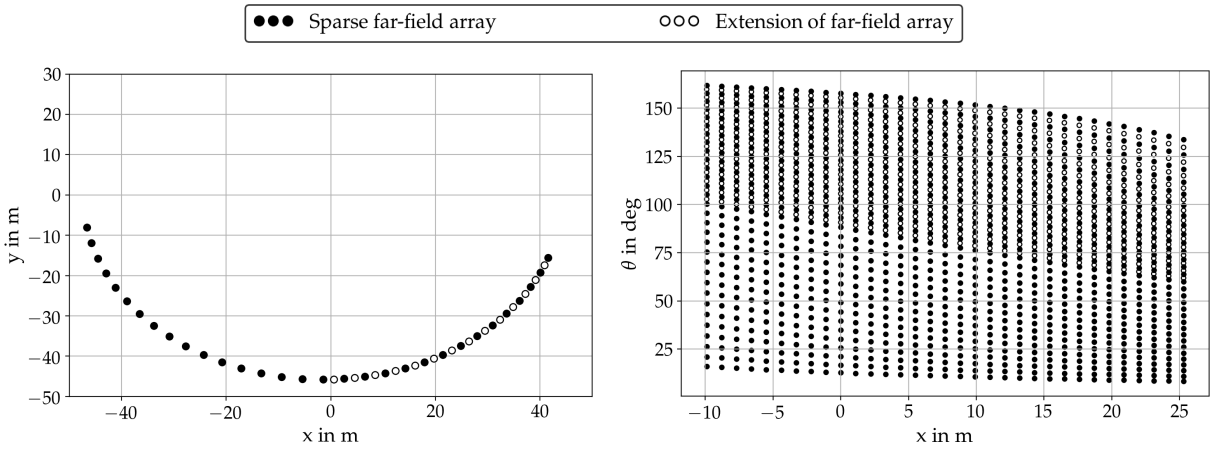

(a) Microphone positions in the far-field

(b) Source points for localisation

Figure 10: Comparison of the sparse far-field array with 31 microphones and the extended array with 14 additional microphones in the rear arc. The increased microphone count leads to a higher resolution in the source grid at high emission angles.

The basic far-field array is extended by 14 additional microphones in the rear arc, such that the spatial density of the array doubles for high emission angles. In this meaning, the sparse far-field array will become more dense, although it remains sparse in comparison to the near-field array with 248 microphones. The extension of the array is realised in the rear arc to take into account the main radiation direction of the distributed jet sources.

Figure 11 shows the source localisation with SODIX and the source breakdown for the basic and the extended far-field array in the 400 Hz one-third octave band. The simulated source positions are roughly marked by the grey dashed lines. The line furthest downstream indicates the end of the simulated jet distribution. For the sparse array, spurious sound sources downstream the jet area appear that are completely eliminated when localised with the extended array. This can be seen as an indication that the phenomenon of the spurious sound sources in the jet area only occurs due to the spatial undersampling with the sparse far-field array. The far-field extrapolation of the source localisation with both arrays shows rather minor differences. Most of all, the application of the extended far-field array leads to a better localisation of the maximum directivity of the nozzle source.

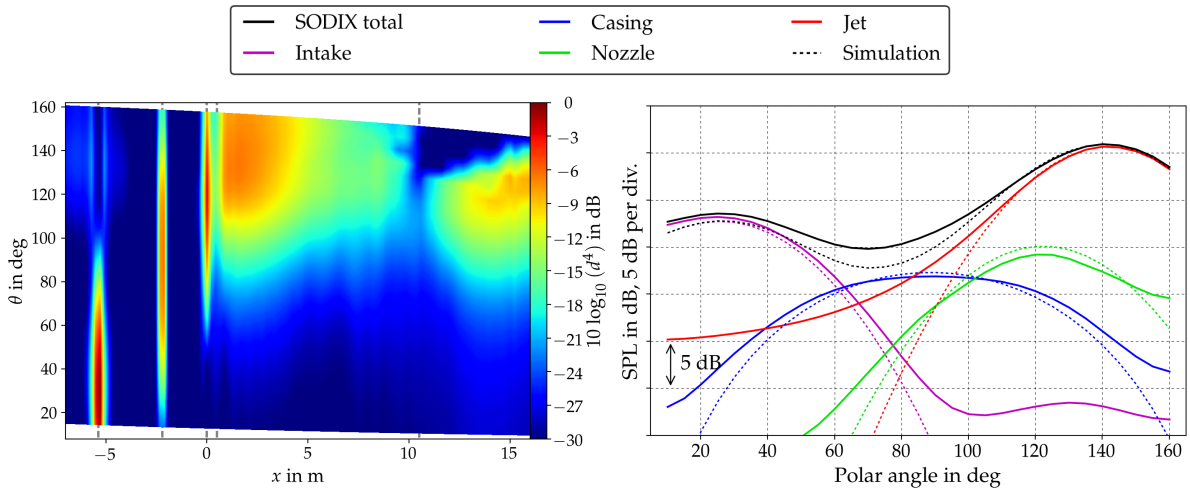

(a) Sparse far-field array with 31 microphones

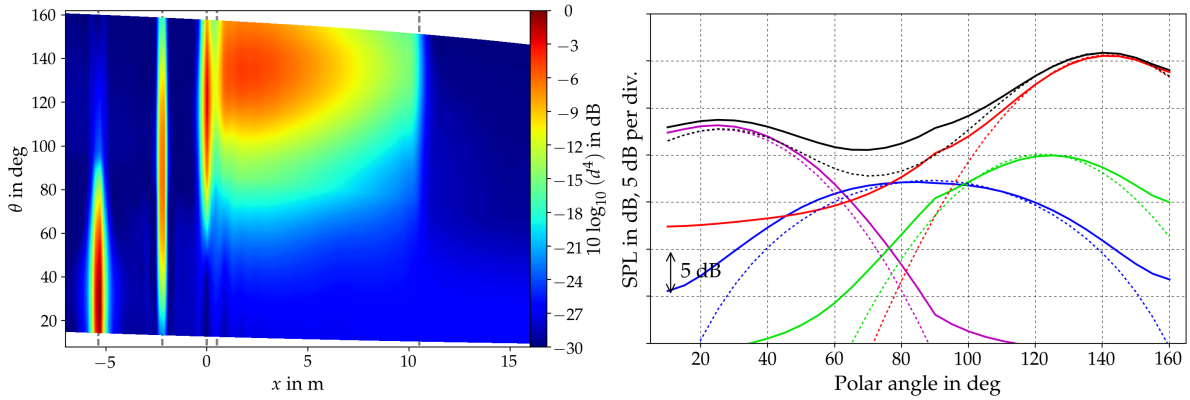

(b) Extended far-field array

Figure 11: Comparison of the source localisation with SODIX and the far-field extrapolation for synthesised sound sources with the sparse far-field array (top) and the extended array (bottom) with 14 additional microphones in the rear arc in the 400 Hz one-third octave band.

5 CONCLUSIONS

In this paper, the source localisation method SODIX was applied to data from a sparse far-field microphone array at a static aero-engine noise test. First, the feasibility of the source localisation with the far-field array was demonstrated. For the frequency range up to 1 kHz, the localisation of the main source regions is in good agreement with the results from the dense microphone array in the near-field. This low to mid frequency range is the most interesting for the separation of broadband noise from a turbofan engine because the sound field is emitted by different distributed sources with strong directivities. For the sparse array, spurious sound sources downstream of the jet area appear in the source maps due to the low spatial sampling of the sound field by the reduced number of microphones in the far-field array. However, the impact on the far-field characteristics of the individual source areas is rather small.

The source localisation method SODIX can be influenced by a penalty function and its two parameters, the penalty coefficient σ_d that is used to weight the penalty function against the raw source localisation and the angular aperture G_ϕ that controls the number of nearby microphones that are taken into account in the penalty function. The impact of the penalty function applied in the localisation algorithm was demonstrated using the experimental data as well as data from a simple engine noise model. The use of the penalty function reduces the spurious sources in the jet area for the measured data. A parametric study of the penalty function was conducted in order to investigate the influence of both parameters. The influence of the parameter G_ϕ on the localisation results is rather small in the examined parameter field. The optimal value for the penalty coefficient σ_d depends on the number of microphones in the array, and the characteristics of the sound sources such as amplitude and directivity, and the overall sound pressure level measured by the microphones. The interaction of all these parameters complicates an accurate normalisation of the penalty function against the raw source localisation.

The results prove that SODIX can be applied to sparse microphone arrays in the far-field. This allows new applications of the source localisation method to existing and future datasets from static aero-engine noise tests. Additionally, an extension of the sparse far-field array was proposed that increases the spatial resolution in the rear arc and therefore eliminates false sources in the jet area.

ACKNOWLEDGEMENTS

The research leading to these results has received funding from the German Federal Ministry for Economic Affairs and Energy (BMWi) in the framework of the LuFo project LIST under the grant agreement number 20T1307B.

REFERENCES

[1] "SAE ARP1846 – Measurement of Far Field Noise from Gas Turbine Engines During Static Operation." SAE International, aerospace recommended practice, 2008.

[2] D. Blacodon and G. Élias. "Level estimation of extended acoustic sources using an array of microphones." In *9th AIAA/CEAS Aeroacoustics Conference and Exhibit, 12-14 May 2003, Hilton Head, South Carolina*, AIAA 2003-3199. 2003.

[3] D. Blacodon and G. Élias. "Level estimation of extended acoustic sources using a parameteric method." *Journal of Aircraft*, 41, 1360–1369, 2004.

[4] S. Funke. *Ein Mikrofonarray-Verfahren zur Untersuchung der Schallabstrahlung von Turbofantriebwerken*. Ph.D. thesis, Technische Universität Berlin, 2017.

[5] S. Funke, R. P. Dougherty, and U. Michel. "Sodix in comparison with various deconvolution methods." In *5th Berlin Beamforming Conference*, BeBeC 2014-11. 2014.

[6] S. Funke, H. A. Siller, W. Hage, and O. Lemke. "Microphone-array measurements of a Rolls-Royce BR700 series aeroengine in an indoor test-bed and comparison with free-field data." In *20th AIAA/CEAS Aeroacoustics Conference, 16-20 Jun 2014, Atlanta, Georgia, USA*, AIAA 2014-3070. 2014.

[7] S. Funke, A. Skorpel, and U. Michel. "An extended formulation of the sodix method with application to aeroengine broadband noise." In *18th AIAA/CEAS Aeroacoustics Conference, 4-6 June 2012, Colorado Springs, USA*, AIAA 2012-2276. 2012.

[8] S. A. L. Glegg. *Jet Noise Source Location*. Ph.D. thesis, University of Southampton, 1979.

[9] G. Herold and E. Sarradj. "An approach to estimate the reliability of microphone array methods." In *21st AIAA/CEAS Aeroacoustics Conference, 22-26 June 2015, Dallas, TX*. 2015.

[10] U. Michel and S. Funke. "Noise source analysis of an aeroengine with a new inverse method sodix." In *14th AIAA/CEAS Aeroacoustics Conference (29th AIAA Aeroacoustics Conference), May 5-7, 2008, Vancouver, British Columbia*, AIAA 2008-2860. 2008.